

Relativistic Green's Function Model and Optical Potential

C. Giusti¹, A. Meucci¹, M.V. Ivanov², J.M. Udías³

¹Dipartimento di Fisica Nucleare e Teorica, Università degli Studi di Pavia and INFN, Sezione di Pavia, via Bassi 6 I-27100 Pavia, Italy

²Institute for Nuclear Research and Nuclear Energy, Bulgarian Academy of Sciences, Sofia 1784, Bulgaria

³Grupo de Física Nuclear, Departamento de Física Atómica, Molecular y Nuclear, Universidad Complutense de Madrid, CEI Moncloa, 28040 Madrid, Spain

Abstract. The relativistic Green's function model describes final-state interactions in the inclusive quasi-elastic lepton-nucleus scattering by means of a complex optical potential. The model has been quite successful in the description of data of electron and neutrino-nucleus scattering, but there are some caveats due to the use of phenomenological optical potentials. We discuss the theoretical uncertainties of the model and present results obtained with a new global relativistic folding optical potential.

1 Introduction

Accurate predictions of neutrino-nucleus cross sections are needed for use in ongoing experimental studies of neutrino oscillations at GeV energies, where nuclei are used as neutrino detectors. A proper analysis of data requires that the nuclear response to neutrino interactions is well under control and that the unavoidable uncertainties on nuclear effects are reduced as much as possible. Several decades of experimental and theoretical work on electron scattering have provided a wealth of detailed information on nuclear structure and dynamics [1, 2]. Models developed and successfully tested in comparison with electron-scattering data have been extended to neutrino-nucleus scattering. Although different, the two situations present many similar aspects, the extension of the formalism to neutrino scattering is straightforward, and the comparison with electron-scattering data represents the first necessary test of a nuclear model. Recently, the MiniBooNE collaboration has produced high-quality data, mostly on a carbon target, for a number of selected channels, in particular, for the Quasi-Elastic (QE) one [3, 4], that is, where no pions are detected in the final state. Within the QE kinematic domain, the nuclear response to the electroweak probe is dominated by the single-particle (s.p.) dynamics, by the process where the probe directly interacts with only one nucleon (in the Impulse Approximation (IA) through a one-body current on a quasi-free nucleon) which is then

knocked out of the nucleus. A proper description of the Final-State Interactions (FSI) between the emitted nucleon and the residual nucleus is very important for a correct interpretation of the experimental data.

In electron-scattering experiments the emitted nucleon can be detected in coincidence with the scattered electron. Kinematic situations can be envisaged where the residual nucleus is left in a discrete eigenstate and the final state is completely determined. This is the exclusive one-nucleon knockout, that is usually described in the Distorted-Wave IA (DWIA), where FSI are accounted for by a complex Optical Potential (OP) whose imaginary part gives an absorption that reduces the calculated cross section. This reduction is essential to reproduce $(e, e'p)$ data [1, 2, 5–9]. In the inclusive scattering only the scattered electron is detected, the final nuclear state is not determined and all available final states are included in the measured cross section. In this case, a model based on the DWIA, where the cross section is given by the sum, over all the nucleons, of integrated one-nucleon knockout processes and FSI are described by a complex OP with an imaginary absorptive part, is conceptually wrong. The OP describes elastic nucleon-nucleus and its imaginary part accounts for the fact that, if other channels are open besides the elastic one, part of the incident flux is lost in the elastically scattered beam and appears in the inelastic channels which are open. This flux may not contribute to the experimental cross section of the exclusive reaction, where only one channel is considered, and the experimental signal receives contributions mainly from the process where the knocked-out nucleon scatters elastically with the residual nucleus in the considered final state. In contrast, in the inclusive scattering the flux lost in a channel must be recovered in the other channels and in the sum over all the channels the flux can be redistributed but must be conserved. The DWIA does not conserve the flux.

In the Relativistic Green's Function (RGF) model FSI are described in the inclusive QE scattering consistently with the exclusive scattering by the same complex OP, but in the inclusive scattering the imaginary part redistributes and conserves the flux in all the final-state channels. The model was originally developed within a nonrelativistic [10, 11] and then within a relativistic framework [12–15] for the inclusive (e, e') scattering. The relativistic model (RGF) was then extended to neutrino-nucleus scattering [16–26]. The formalism can translate the flux lost toward inelastic channels, represented by the imaginary part of the OP, into the strength observed in inclusive reactions. Therefore, the OP becomes a powerful tool to include, in a relatively simple and somewhat less model dependent way than with microscopic calculations, important contributions not included in other descriptions of FSI based in the IA. The model has been quite successful in the comparison with data: it provides a good description of QE (e, e') data and of the Charged-Current QE (CCQE) MiniBooNE and MINER ν A data, both for neutrino and antineutrino scattering [3, 4, 20, 22, 26–28], and of Neutral-Current Elastic (NCE) MiniBooNE data [21, 25, 29, 30].

The model is successful but there are some caveats. The availability of phenomenological OPs makes RGF calculations feasible, but the use of a phe-

phenomenological potential does not allow us to disentangle and evaluate the role of a specific contribution: all inelastic contributions are included, all together, in the imaginary part of the OP. Phenomenological OPs are obtained through a fit to elastic proton-nucleus scattering data. Available data, however, do not completely constrain the shape and the size of the OP. Different phenomenological OPs are available, they are able to give practically equivalent descriptions of elastic proton-scattering data but they are different, in particular, in their imaginary parts. Different imaginary parts can give different inelastic contributions and, therefore, different results in RGF calculations. These differences may introduce theoretical uncertainties on the numerical predictions of the model.

In this contribution we discuss the uncertainties due to the use of the OP in RGF calculations. In particular, we present results obtained with a new microscopic Global Relativistic Folding OP (GRFOP) [31, 32] generated within the Relativistic IA (RIA) by folding the Horowitz-Love-Franey (HLF) [33, 34] t -matrix with the relevant relativistic mean-field Lorentz densities via the so-called $t\rho$ -approximation. The new results are compared with previous results obtained with phenomenological OPs [35].

2 Relativistic Green's Function Model

Lepton-nucleus scattering is usually described in the one-boson exchange approximation, where the cross section is obtained from the contraction between the lepton tensor, which essentially depends on the lepton kinematics, and the hadron tensor $W^{\mu\nu}$, whose components are given by products of the matrix elements of the nuclear current between the initial and final nuclear states.

In the RGF model with suitable approximations, which are mainly related to the IA, the components of the hadron tensor are written in terms of the s.p. optical model Green's function. The explicit calculation of the s.p. Green's function can be avoided by its spectral representation, which is based on a biorthogonal expansion in terms of the eigenfunctions of the non-Hermitian optical potential and of its Hermitian conjugate

$$[\mathcal{E} - T - \mathcal{V}^\dagger(E)] | \chi_{\mathcal{E}}^{(-)}(E) \rangle = 0, \quad [\mathcal{E} - T - \mathcal{V}(E)] | \tilde{\chi}_{\mathcal{E}}^{(-)}(E) \rangle = 0. \quad (1)$$

The expanded form for the s.p. expression of the hadron tensor is [12, 16]

$$W^{\mu\nu}(q, \omega) = \sum_n \left[\text{Re } T_n^{\mu\nu}(E_f - \varepsilon_n, E_f - \varepsilon_n) - \frac{1}{\pi} \mathcal{P} \int_M^\infty d\mathcal{E} \frac{1}{E_f - \varepsilon_n - \mathcal{E}} \text{Im } T_n^{\mu\nu}(\mathcal{E}, E_f - \varepsilon_n) \right], \quad (2)$$

where \mathcal{P} denotes the principal value of the integral, n is the eigenstate of the

residual nucleus, with energy ε_n , and

$$T_n^{\mu\mu}(\mathcal{E}, E) = \lambda_n \langle \varphi_n | j^{\mu\dagger}(\mathbf{q}) \sqrt{1 - \mathcal{V}'(E)} | \tilde{\chi}_{\mathcal{E}}^{(-)}(E) \rangle \\ \times \langle \chi_{\mathcal{E}}^{(-)}(E) | \sqrt{1 - \mathcal{V}'(E)} j^{\mu}(\mathbf{q}) | \varphi_n \rangle, \quad (3)$$

and similar expressions for the terms with $\mu \neq \nu$. The factor $\sqrt{1 - \mathcal{V}'(E)}$, where $\mathcal{V}'(E)$ is the energy derivative of the OP, accounts for interference effects between different channels and allows the replacement of the mean field \mathcal{V} with the phenomenological OP.

Disregarding the square-root correction, the second matrix element in Eq. (3) is the transition amplitude for the one-nucleon knockout where the residual nucleus is left in the state $|n\rangle$ and it is similar to the DWIA transition amplitude of the exclusive scattering, i.e., the imaginary part of \mathcal{V}^\dagger gives an attenuation of the strength that is inconsistent with the inclusive process where, in the sum over all the channels, the total flux must be conserved. The compensation is performed by the first matrix element of Eq. (3), which involves the eigenfunction $\tilde{\chi}_{\mathcal{E}}^{(-)}(E)$ of the Hermitian conjugate OP, where the imaginary part has an opposite sign and increases the strength. Therefore, in the RGF the imaginary part of the OP redistributes the flux lost in a channel in the other channels, and in the sum over n the total flux is conserved.

The RGF model gives a good description of the experimental (e, e') cross sections in the QE region, in particular, in kinematic situations where the longitudinal response is dominant [12, 14, 15]. In the case of neutrino scattering the model is able to describe CCQE and NCE MiniBooNE data and CCQE Minerva data [20–22, 25, 26]. In comparison with the MiniBooNE cross sections the RGF results are usually larger than the results of other models based on the IA, which, in general, underpredict data. The enhancement can be ascribed to the overall effect of the inelastic channels, which are recovered in the RGF model by the imaginary part of the relativistic OP and that are not included in other models based on the IA.

The OP can recover, to some extent, contributions beyond direct one-nucleon emission, such as, for instance, rescattering of the outgoing nucleon and some multinucleon processes, which can be included in CCQE measurements. The model, being based on the use of a one-body nuclear current, does not contain meson-exchange-currents mechanisms that can be included in CCQE data and that in other models have been found to be significant. On the other hand, the OP can include pion-absorption and pion-emission processes, that should have already been subtracted in the MiniBooNE analysis. With a phenomenological OP we cannot disentangle the role of a specific reaction process, such as, for instance, possible pion contribution. It has been written in [37] that the good agreement of the RGF results with the MiniBooNE data “should be interpreted with care” and that “it would be very interesting to confront the RGF results with the fully CC-inclusive data”, where pion production is included.

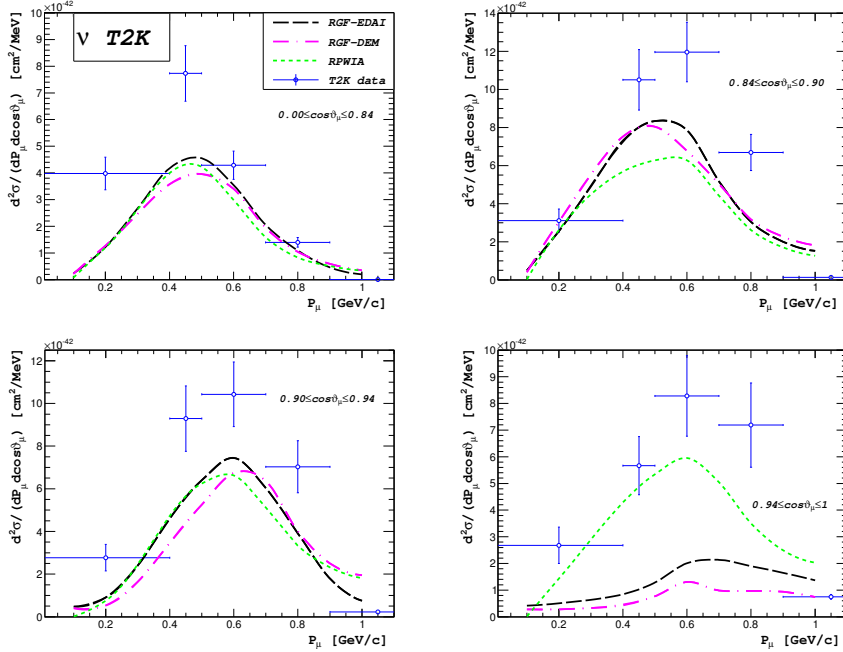


Figure 1. Flux-averaged CC-inclusive double differential ν_μ - ^{12}C cross sections per target nucleon as a function of the muon momentum. The data are from T2K [38].

The comparison with the fully CC-inclusive double differential cross sections on ^{12}C measured by the T2K collaboration [38] is shown in Figure 1, for four different bins in the scattering angle. For the RGF calculations two different parametrizations for the relativistic OP of ^{12}C have been adopted: the Energy-Dependent and A-Independent EDAI OP of [35] and the more recent Democratic (DEM) OP of [39]. The EDAI OP is a single-nucleus parametrization, which is constructed to better reproduce the elastic proton- ^{12}C phenomenology, whereas DEM depends on the atomic number A and is obtained through a fit to more than 200 data sets of elastic proton-nucleus scattering data on a wide range of nuclei. The results of the Relativistic Plane-Wave IA (RPWIA), where FSI are neglected, also shown in the figure, are approximately 50% lower than the data. Both RGF results are also generally lower than the data, although within the error bars for low values of the muon momentum and large angular bins. In the RGF the imaginary part of the OP can include the excitation of multinucleon channels. We cannot exclude that it can contain some contribution due to pion emission, but the results in Figure 1 indicate that this is not enough to reproduce CC-inclusive data. A satisfactory agreement with the data is obtained with the model of [40], which includes np-nh excitations and single-pion production. The comparison with [40] gives a clear indication that full np-nh excitations and

single-pion production are not included in the RGF calculations [41]. This result reinforces the validity of the RGF as a model suitable for QE scattering.

3 Global Relativistic Folding Optical Potential

The predictions of the RGF model can be affected by uncertainties due to the use of different phenomenological OPs. To reduce such uncertainties and to ascertain to what extent the RGF predictions can be relied upon, the need arises to build microscopic relativistic OPs. As an alternative to the use of purely phenomenological potentials, a new relativistic OP has been built for ^{12}C , a nucleus that is often used in neutrino-scattering experiments. The new OP is global, just like the phenomenological OPs used in previous RGF calculations, *i.e.*, spanning a large range of kinetic energies of the nucleon, and it has been built from a folding approach [31, 32]. In this way the shape of the potential is severely constrained by the assumed shape of the nuclear density and the strength of the different contributions, in particular the real and imaginary parts, is essentially dictated by their respective contents in the effective parametrization of the NN scattering amplitudes. Indeed, within the Relativistic IA (RIA), one can build OPs to study nucleon-nucleus reactions which provide excellent quantitative descriptions of complete sets of elastic proton-scattering observables from various spin-saturated spherical nuclei [33, 34]. Two basic ingredients underly the realization of these folding potentials: a suitable analytical representation for the NN -interaction and an appropriate relativistic model of nuclear densities. The new Global Relativistic Folding OP (GRFOP) has been generated by folding the Horowitz-Love-Franey (HLF) t -matrix with the relevant relativistic mean-field Lorentz densities via the so-called $t\rho$ -approximation.

In comparison with the phenomenological OPs the new GRFOP: 1) is derived from all available experimental data of elastic proton scattering on ^{12}C we are aware of; 2) stems from a folding approach, with neutron density fitted to data and proton density taken from electron-scattering experiments; 3) the same nuclear densities are used at all the energies in the range between 20 and 1040 MeV; 4) the imaginary term is built from the effective NN interaction.

The GRFOP is able to reproduce quite well the energy dependence of the experimental differential cross sections for the elastic proton scattering on ^{12}C in the energy range between 20 and 1040 MeV [32]. Also the calculated analyzing powers are in good agreement with the data [32]. The agreement is comparable to the one obtained with the phenomenological EDAI and EDAD1 potentials [35]. For the three OPs the values of χ^2 per degree of freedom, obtained from the comparison with all available experimental data of elastic proton scattering, are: 2.2 (EDAI), 4.7 (GRFOP), 5.6 (EDAD1).

The GRFOP has been tested within the RGF for QE electron scattering and $\nu(\bar{\nu})$ -nucleus scattering at MiniBooNE kinematics [32]. In the case of electron scattering the results are in generally good agreement with the experimental (e, e') cross sections and close to the results obtained with EDAI and

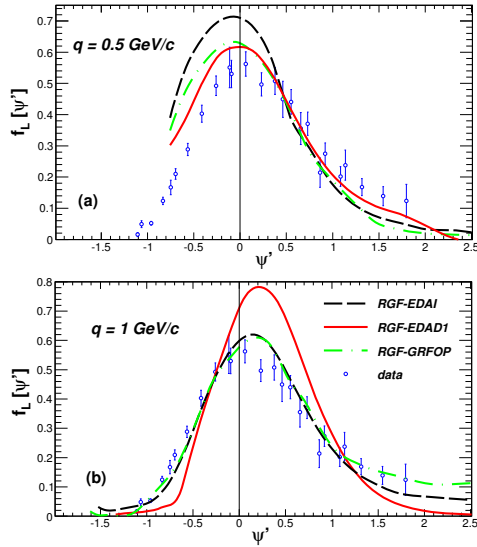


Figure 2. Longitudinal contributions to the scaling function for $q = 500$ and 1000 MeV/ c compared with the averaged experimental scaling function.

EDAD1 [32]. Of particular interest is the comparison with the experimental longitudinal scaling function. The analysis of QE (e, e') world data has shown that these data, when plotted against a properly chosen scaling variable Ψ' , show a mild dependence on the momentum transfer (scaling of first kind) and almost no dependence on the nuclear target (scaling of second kind). These properties are well satisfied in the longitudinal channel, while violations associated to effects beyond the IA occur mainly in the transverse channel [42,43]. The scaling function is obtained dividing the longitudinal contribution to the (e, e') cross sections by an appropriate single-nucleon cross section [42,44]. In Figure 2 the scaling functions obtained in the RGF with the RGFOP, EDAI, and EDAD1 OPs for two values of the momentum transfer q are compared with the experimental function. The asymmetric shape of the experimental function is reproduced by the RGF model. The different dependence on q of the results with the three OPs makes the RGF scaling-function tail less pronounced as the value of q goes up. It is interesting to notice the different behavior as a function of q of the results with EDAI and EDAD1 in comparison with the experimental function: EDAD1 reproduces the experimental function at $q = 0.5$ GeV/ c and overestimates it at $q = 1$ GeV/ c , while with EDAI the experimental function is overestimated at $q = 0.5$ GeV/ c and reproduced at $q = 0.5$ MeV/ c . The RGF results with these two OPs do not scale enough. In contrast, the results with RGFOP scale better, they give a milder dependence on q and a better agreement with the experimental scaling function.

The Relativistic Green's Function Model and the Optical Potential

The comparison of the RGF results with CCQE MiniBooNE data is presented in Figure 3, where the flux-averaged double-differential cross sections per target nucleon for ν and $\bar{\nu}$ scattering are plotted as functions of the muon

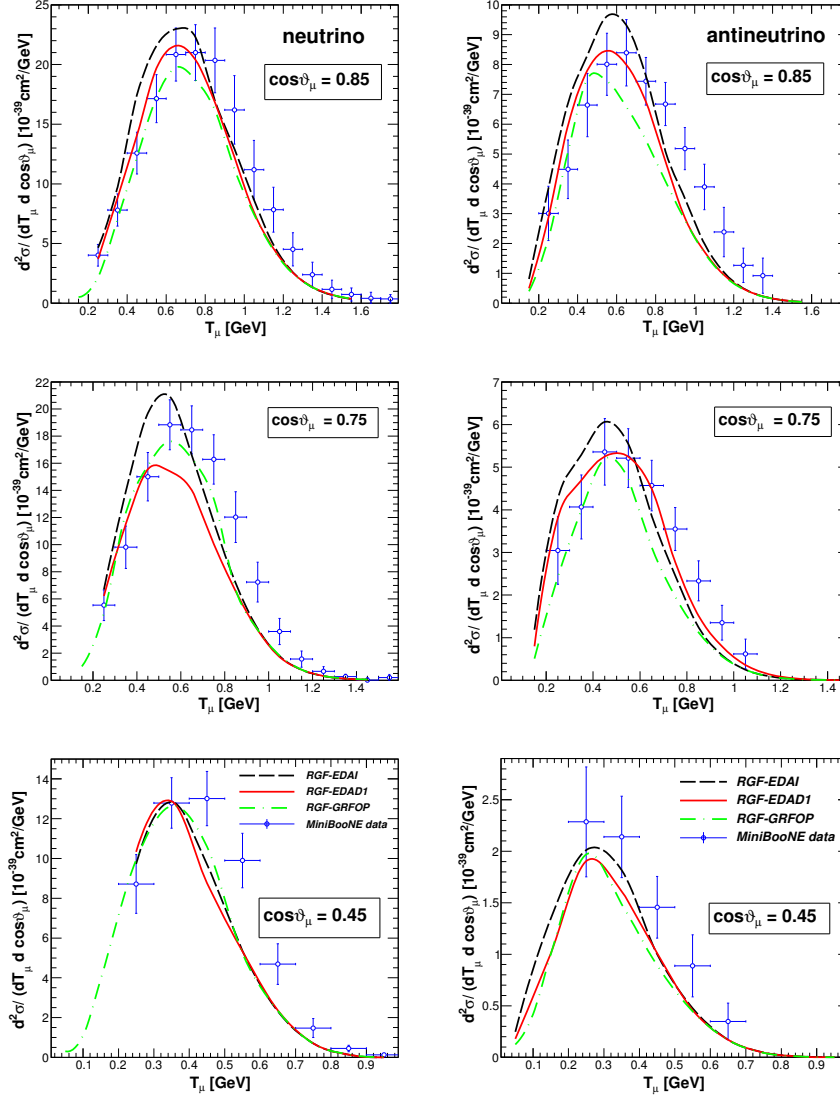


Figure 3. [] Flux-averaged double-differential cross section per target nucleon for the CCQE $^{12}\text{C}(\nu_{\mu}, \mu^{-})$ (left panels) and $^{12}\text{C}(\bar{\nu}_{\mu}, \mu^{-})$ (right panels) reactions as a function of the muon kinetic energy T_{μ} for three bins of the muon scattering angle $\cos \vartheta_{\mu}$ calculated with RGF-GRFOP (dot-dashed lines), RGF-EDAD1 (solid lines) and RGF-EDAI (dashed lines). Experimental data from MiniBooNE [3,4].

kinetic energy T_μ for three bins of the muon scattering angle ϑ_μ . A good agreement with the shape of the experimental cross sections is generally obtained with all the three OPs. The RGF-EDAD1 and RGF-EDAI results are similar in the bin $0.4 \leq \cos \vartheta_\mu \leq 0.5$. Larger differences, around 20%, are obtained in the peak region for the forward-angle scattering bins, the RGF-EDAI results being larger than the RGF-EDAD1 ones and also in somewhat better agreement with the neutrino-scattering data. In the case of antineutrino scattering, data are slightly overestimated by the RGF-EDAI calculations and satisfactorily described by RGF-EDAD1. The RGF-GRFOP results are always smaller than the RGF-EDAI and the RGF-EDAD1 ones for the bin $0.8 \leq \cos \vartheta_\mu \leq 0.9$, while for the bin $0.7 \leq \cos \vartheta_\mu \leq 0.8$ they are larger than the RGF-EDAD1 results and in better agreement with the data. Similar results in comparison with data are produced by the three RGF calculations for the bin $0.4 \leq \cos \vartheta_\mu \leq 0.5$.

The MiniBooNE collaboration has also reported [29, 30] a measurement of the NCE flux-averaged differential ν and $\bar{\nu}$ cross section on CH_2 as a function of the four-momentum transferred squared Q^2 , where $Q^2 = 2m_N \sum_i T_i$, m_N is the nucleon mass and $\sum_i T_i$ is the total kinetic energy of the outgoing nucleons. The comparison of NCE data with the RGF results is shown in Figure 4. In the case of neutrino scattering the RGF-EDAI results reproduce the shape and the magnitude of the experimental cross section, but overestimate the first datum at the smallest value of Q^2 ; the RGF-EDAD1 results underestimate the data only at the smallest values of Q^2 considered in the figure; the RGF-GRFOP calculations generally provide a satisfactory agreement with the data. Also in the case of antineutrino scattering the RGF results are in satisfactory agreement with the data. Close results, in the entire kinematical range of the MiniBooNE $\bar{\nu}$ flux, are obtained with RGF-EDAD1 and RGF-GRFOP, while the RGF-EDAI cross

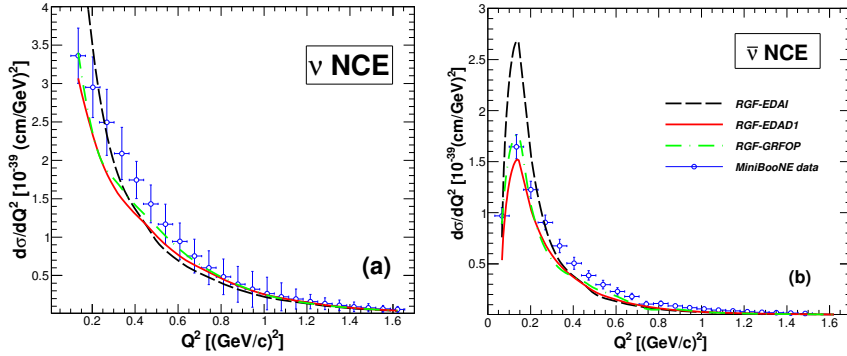


Figure 4. (Neutrino and antineutrino NCE flux-averaged cross section per target nucleon as a functions of Q^2 calculated with RGF-GRFOP (dot-dashed lines), RGF-EDAD1 (solid lines), and RGF-EDAI (dashed lines). Experimental data from MiniBooNE [29, 30].

The Relativistic Green's Function Model and the Optical Potential

section is enhanced at $Q^2 \approx 0.1$ (GeV/c)². All the RGF results are able to reasonably reproduce the first datum at $Q^2 \approx 0.06$ (GeV/c)².

The RGF-GRFOP results lie, in general, between the RGF-EDAI and RGF-EDAI ones and are in many cases in better agreement with the experimental data. The new GRFOP results reduce the uncertainties in the numerical predictions of the RGF model and confirm our previous findings in comparison with data. The RIA can provide successful relativistic OPs with similar fits to elastic nucleon-nucleus scattering data. The GRFOP can be employed as a useful alternative to phenomenological OPs. In the present application it has been employed in the RGF model, where the OP is the basic ingredient, but its use can be extended to calculations for a wide variety of nuclear reactions where the OP is crucial and critical input.

References

- [1] S. Boffi, C. Giusti, and F.D. Pacati, *Phys. Rep.* **226** (1993) 1-101.
- [2] S. Boffi, C. Giusti, F.D. Pacati, and M. Radici, “*Electromagnetic Response of Atomic Nuclei*”, Oxford Studies in Nuclear Physics, Vol. 20 (Clarendon Press, Oxford, 1996).
- [3] A.A. Aguilar-Arevalo *et al.*, *Phys. Rev. D* **81** (2010) 092005-1-22.
- [4] A.A. Aguilar-Arevalo *et al.*, *Phys. Rev. D* **88** (2013) 032001-1-22.
- [5] J.M. Udías, P. Sarriguren, E. Moya de Guerra, E. Garrido, and J.A. Caballero, *Phys. Rev. C* **48** (1993) 2731-2739.
- [6] A. Meucci, C. Giusti, and F.D. Pacati, *Phys. Rev. C* **64** (2001) 014604-1-10.
- [7] A. Meucci, C. Giusti, and F.D. Pacati, *Phys. Rev. C* **64** (2001) 064615-1-8.
- [8] M. Radici, A. Meucci, and W.H. Dickhoff, *Eur. Phys. J. A* **17** (2003) 65-69.
- [9] C. Giusti, A. Meucci, C. Giusti, F.D. Pacati, G. Co’, and V. De Donno, *Phys. Rev. C* **84** (2011) 024615-1-12.
- [10] F. Capuzzi, C. Giusti, and F.D. Pacati *Nucl. Phys. A* **524** (1991) 681-705.
- [11] F. Capuzzi, C. Giusti, F.D. Pacati, and D.N. Kadrev, *Ann. Phys.* **317** (2005) 492-529.
- [12] A. Meucci, F. Capuzzi, C. Giusti, and F.D. Pacati, *Phys. Rev. C* **67** (2003) 054601-1-12.
- [13] A. Meucci, C. Giusti, and F.D. Pacati, *Nucl. Phys. A* **756** (2005) 359-381.
- [14] A. Meucci, J.A. Caballero, C. Giusti, F.D. Pacati, and J.M. Udías, *Phys. Rev. C* **80** (2009) 024605-1-12.
- [15] A. Meucci, M. Vorabbi, C. Giusti, F.D. Pacati, and P. Finelli, *Phys. Rev. C* **87** (2013) 054620-1-14.
- [16] A. Meucci, C. Giusti, and F.D. Pacati, *Nucl. Phys. A* **739** (2004) 277-290.
- [17] A. Meucci, C. Giusti, and F.D. Pacati, *Acta Phys. Polon. B* **37** (2006) 2279-2286.
- [18] A. Meucci, C. Giusti, and F.D. Pacati, *Acta Phys. Polon. B* **40** (2009) 2579-2584.
- [19] A. Meucci, J.A. Caballero, C. Giusti, F.D. Pacati, and J.M. Udías, *Phys. Rev. C* **83** (2011) 064614-1-10.
- [20] A. Meucci, M.B. Barbaro, J.A. Caballero, C. Giusti C, and J.M. Udías, *Phys. Rev. Lett.* **107** (2011) 172501-1-5.
- [21] A. Meucci, C. Giusti, and F.D. Pacati, *Phys. Rev. D* **84** (2011) 113003-1-8.

- [22] A. Meucci, and C. Giusti, *Phys. Rev. D* **85** (2012) 093002-1-6.
- [23] A. Meucci, C. Giusti, and M. Vorabbi, *Phys. Rev. D* **88** (2013) 013006-1-7.
- [24] R. González-Jiménez, J.A. Caballero, A. Meucci, C. Giusti, M.B. Barbaro, M.V. Ivanov, and J.M. Udías, *Phys. Rev. C* **88** (2013) 025502-1-10.
- [25] A. Meucci, and C. Giusti, *Phys. Rev. D* **89** (2014) 057302-1-4.
- [26] A. Meucci, and C. Giusti, *Phys. Rev. D* **88** (2014) 117301-1-5.
- [27] G.A. Fiorentini *et al.*, *Phys. Rev. Lett.* **111** (2013) 022502-1-6.
- [28] L. Fields *et al.*, *Phys. Rev. Lett.* **111** (2013) 022501-1-7.
- [29] A.A. Aguilar-Arevalo *et al.*, *Phys. Rev. D* **82** (2010) 092005-1-16.
- [30] A.A. Aguilar-Arevalo *et al.*, *Phys. Rev. D* **91** (2015) 092005-1-12.
- [31] M.V. Ivanov, J.R. Vignote, R. Álvarez-Rodríguez, and J.M. Udías *Nuclear Theory* **30** (2011) 116-125, eds. A.I. Georgieva and N. Minkov (Heron Press, Sofia).
- [32] M.V. Ivanov, J.R. Vignote, R. Álvarez-Rodríguez, A. Meucci, C. Giusti, and J.M. Udías *Phys. Rev. C* to be published.
- [33] C.J. Horowitz, *Phys. Rev. C* **31** (1985) 1340-1348.
- [34] D.P. Murdock and C.J Horowitz, *Phys. Rev. C* **35** (1987) 1442-1462.
- [35] E.D. Cooper, S. Hama, B.C. Clark, and R.L. Mercer, *Phys. Rev. C* **47** (1993) 297-311.
- [36] Y. Horikawa, F. Lenz, and N.C. Mukhopadhyay, *Phys. Rev. C* **22** (1980) 1680-1695.
- [37] L. Alvarez-Ruso, Y. Hayato, and J. Nieves, *New. J. Phys* **16** (2014) 075015-1-63.
- [38] K. Abe *et al.*, *Phys. Rev. D* **87** (2013) 092003-1-20.
- [39] E.D. Cooper, S. Hama, and B.C. Clark, *Phys. Rev. C* **80** (2009) 034605-1-5.
- [40] M. Martini and M. Ericson, *Phys. Rev. C* **90** (2014) 025501-1-6.
- [41] A. Meucci and C. Giusti, *Phys. Rev. D* **91** (2015) 093004-1-6.
- [42] C. Maieron, T.W. Donnelly, and I. Sick, *Phys. Rev. C* **65** (2002) 025502-1-15.
- [43] T.W. Donnelly and I. Sick, *Phys. Rev. Lett.* **82** (1999) 3212-3215; *Phys. Rev. C* **60** (1999) 065502-1-16.
- [44] J.A. Caballero, *Phys. Rev. C* **74** (2006) 015502-1-12.